Dynamic Response of Layered Cohesive Soil

By

Fusao OKA*

(Received March 30, 1978)

Abstract

The realistic stress-strain relation of cohesive soil is applied to analyze the dynamic response of layered cohesive soil system during shear wave propagation. The cohesive soil is treated as a saturated elastic-viscoplastic body and assumed to be a K_0-consolidated state. The characteristics method was used for this anaysis, and the stress, strain and velocity under the ground were determined from the surface motion. From the analytical result, even if the surface response is the same between the elastic ground and elastic-viscoplastic ground, the stress, strain and velocity responses of the elastic-viscoplastic ground are greater than those of the elastic ground.

1. Introduction

Faced with the problem of dynamic analysis of ground during earthquakes, these four following factors are considered to be important.

(1) Constitutive equation of soil composing the ground

(2) Boundary conditions (the geological conditions of the site in question)

(3) Type of seismic wave

(4) Method of analysis

This paper considers the influence of the non-linear soil behavior of the dynamic response of layered soil on the basis of the constitutive theory proposed by author[1].

The constitutive equations used for describing the dynamic behavior of soil are as follows: linear elasticity, non-linear elasticity, visco-elasticity and simple elastic-plasticity. The convienient stress-strain relation developed by Ramberg-Osgood is also used by many investigators[2),3)]. On the other hand, the dynamic property of soil has been examined in detail and the constitutive equation that includes the effect of dilatancy is now being established in soil mechanics. Therefore, it is required and of interest to apply these refined constitutive theories to the practical

* Department of Transportation Engineering

problem. Generally, the local geological condition is often inspected in detail. Therefore, a one-dimensional horizontally layered system of the ground is rather easily investigated. Furthermore, a two- or three-dimensional model of ground must be included in the dynamic analysis in the future. When we deal with the wave which has the component of the short period, the dynamic response is sensitive to the local geological system in a surface layer of ground.

To analyze the dynamic behavior of soil deposit in a case where the soil can be described by a unique constitutive equation, two types of methods for analysis exist. One is to describe the soil system as the multi-degree of freedom. Idriss & Seed[4] used a shear beam as a discrete system for computing the ground vibration. This method is called a lumped mass method. This simple method, however, is not convenient for expressing the geometrical dissipation. The other method[3],[5] is to get a solution by integrating a differential relation along the characteristics of partial differential equations. The well used multiple reflection theory of wave is based on this characteristics method. This method is restricted to the linear elastic system. The general characteristics method is available for non-linear analysis, and the time required for computation is relatively short. When the geological condition is complicated and the constitutive equation is not unique, the finite element method is available for analysis. The analysis by the finite element method has a difficulty in determining a boundary condition.

Many seismic records were obtained on the surface of the ground, but the records of base rock motion are scanty. In order to design an underground structure, it is necessary to estimate the strain, velocity or stress under the ground. In this paper, the author aims to determine the strain, stress and velocity in the layered cohesive soil calculated from the surface motion of the ground. The stress-strain relation proposed by the author[1] is extended to the K_0-consolidated condition. The pore-water pressure is also calculated.

2. Ground Model and Equation of Motion

The dynamic response of a horizontally layered system, which is composed of elastic layers and saturated clay layers, will be considered in this paper. Shearing stresses are set up by horizontal motions imposed at the base of soil layer as shown in Fig. 1. The clay layer is initially K_0-consolidated. Fig. 2 shows the initial stress conditions, where $\sigma'_{ij(0)}$ is the initial effective stress. The material property of each layer is assumed to be constant. As the boundary condition, the shear stress at the ground surface is zero and the velocity records at the surface are given. It is important to determine the value of the stress, velocity and strain in the ground, from the ground surface records. The initial stress condition is given as follows.

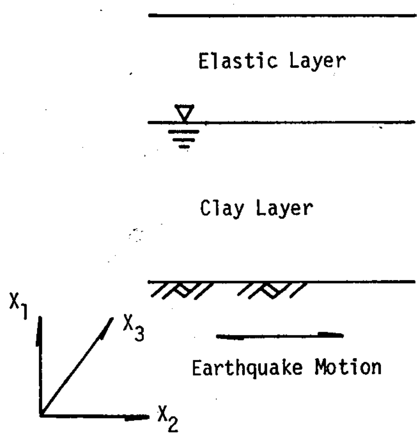

Fig. 1 Model of soil layers.

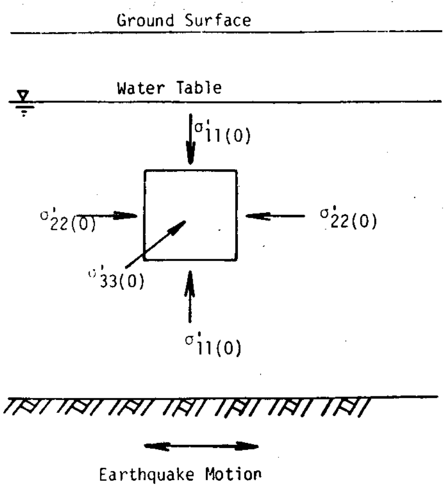

Fig. 2 Stress condition.

$$\sigma'_{ij(0)}=\begin{vmatrix}\sigma_{11(0)} & 0 & 0\\ 0 & K_0\sigma'_{11(0)} & 0\\ 0 & 0 & K_0\sigma'_{11(0)}\end{vmatrix} \tag{1}$$

From Eq. (1), the initial mean effective stress $\sigma'_{m(0)}$ is expressed by

$$\sigma'_{m(0)}=\frac{1}{3}(1+2K_0)\sigma'_{11(0)} \tag{2}$$

Similarly, the initial deviatoric stress $s_{ij(0)}$ is

$$s_{ij(0)}=\begin{vmatrix}\frac{2}{3}(1-K_0)\sigma'_{11(0)} & 0 & 0\\ 0 & \frac{1}{3}(K_0-1)\sigma_{11(0)} & 0\\ 0 & 0 & \frac{1}{3}(K_0-1)\sigma'_{11(0)}\end{vmatrix} \tag{3}$$

$$\begin{aligned}\sqrt{2J_{2(0)}}&=\sqrt{s_{ij(0)}s_{ij(0)}}\\ &=\sqrt{\frac{\sigma'^2_{ij(0)}}{9}[(2-2K_0)^2+2(K_0-1)^2]}\end{aligned} \tag{4}$$

in which, J_2 is the second invariant of the deviatoric stress. The stress condition during the shear wave transmission is given by

$$\sigma'_{ij}=\sigma'_{ij(0)}+\Delta\sigma'_{ij} \tag{5}$$

$$\sigma'_m=\sigma_{ij(0)}+\Delta\sigma'_m \tag{6}$$

$$s_{ij}=s_{ij(0)}+\Delta s_{ij} \tag{7}$$

The equation of motion and the kinetic relation between the strain and the displacement are expressed by Eqs. (8) and (9), respectively.

$$\rho\frac{\partial v_2}{\partial t}=-\left(\frac{\partial\sigma_{21}}{\partial x_1}+\frac{\partial\sigma_{22}}{\partial x_2}+\frac{\partial\sigma_{23}}{\partial x_3}\right) \tag{8}$$

$$-\varepsilon_{12}=\frac{1}{2}\left(\frac{\partial u_2}{\partial x_1}+\frac{\partial u_1}{\partial x_2}\right) \tag{9}$$

Where, the strain tensor ε_{ij} is taken positively in compression and the body force is neglected, v_i; velocity vector, u_i; displacement vector, σ_{ij}; stress tensor, ρ; density of saturated soil. Since derivative components in the x_2 and x_3 direction in the above equations may be negligibly small in one-dimensional analysis, Eqs. (8) and (9) are approximated by Eqs. (10) and (11).

$$\rho\frac{\partial v_2}{\partial t}=-\frac{\partial\sigma_{21}}{\partial x_1} \tag{10}$$

$$-\varepsilon_{12}=\frac{1}{2}\frac{\partial u_2}{\partial x_1} \tag{11}$$

3. Stress-Strain Relation of Soil

The elastic layers are modelled by a linear elastic body expressed by

$$\sigma_{ij}=\bar{\lambda}\varepsilon_{kk}\delta_{ij}+2\bar{\mu}\varepsilon_{ij} \tag{12}$$

where $\bar{\lambda}$ and $\bar{\mu}$ are Lamé's constants.

When $\varepsilon_{kk}=0$, $\sigma_{ij}=2\bar{\mu}\varepsilon_{ij}$. (13)

In the saturated clay layers, the stress-strain relation is presented by an elastic-viscoplastic or viscoelastic-viscoplastic body. We extend the stress-strain relation proposed by the author[1] to an anisotropically consolidated state, and it can be expressed by the following relation in a K_0-consolidated state.

$$\dot{\varepsilon}_{ij}=\gamma_1\dot{s}_{ij}+\frac{1}{3}\gamma_2\dot{\sigma}'_m\delta_{ij}+\beta_1\frac{s_{ij}}{\sqrt{2J_2}}+$$
$$+\beta_2\left[M^*-\frac{\sqrt{2J_2}^{(s)}}{\sigma'^{(s)}_m}+M^*\ln\{\sigma'_m/\sigma'^{(s)}_m\}\right]\frac{1}{3}\delta_{ij} \tag{14}$$

Deduction of Eq. (14) is now given as follows. Roscoe's original theory which was extended to a three-dimensional problem is also formally extended to an anisotropic consolidated state for the purpose of being used in an equilibrium state. The static yield function is given by

$$f_s=\pm(\eta^*-\eta^*_{(0)})+M^*\ln(\sigma'_m/\sigma'_{my})=0 \tag{15}$$

where $\eta^*_{(0)}=\sqrt{2J_{2(0)}}/\sigma'_{m(0)}$. The plus or minus sign of Eq. (15) corresponds to an active or passive state, respectively.

The hardening rule is expressed by

$$\sigma'_m=\sigma'_{me}\exp\left[\frac{1+e}{\lambda-\kappa}\varepsilon^p_{kk}\right] \tag{16}$$

As we postulated that $de=0$ during the wave propagation, the equation is obtained in an equilibrium state according to Adachi & Okano[6] as follows;

$$\lambda\frac{d\sigma'_m}{\sigma'_m}=-\frac{\lambda-\kappa}{M^*}d\eta^* \tag{17}$$

$$d\varepsilon^p_{kk}=\frac{\lambda-\kappa}{1+e}\left[\frac{1}{M^*}d\eta^*+\frac{d\sigma'_m}{\sigma'_m}\right] \tag{18}$$

The plastic volumetric strain increment is given by Eq. (18). From Eqs. (17) and (18), we obtain under the condition of $\eta^*=\eta^*_{(0)}$ when $\varepsilon^p_{kk}=0$,

$$\pm(\eta^*-\eta^*_{(0)})=\frac{(1+e)M^*\lambda}{(\lambda-\kappa)\kappa}\varepsilon^p_{kk} \tag{19}$$

From Eqs. (17) and (19), σ'_m can be determined by

$$\sigma_{m(s)}=\sigma'_{me}\exp\left[-\frac{(1+e)}{\kappa}\varepsilon^p_{kk}\right] \tag{20}$$

Finally, $\sqrt{2J_2}^{(s)}$ is determined by Eqs. (16), (19) and (20).

$$\sqrt{2J_2}^{(s)}=\left[\frac{\sqrt{2J_{2(0)}}}{\sigma'_{m(0)}}\pm\frac{(1+e)M^*\lambda}{(\lambda-\kappa)\kappa}\varepsilon^p_{kk}\right]\sigma'_{m(s)} \tag{21}$$

Therefore, the static stress path in the $\sqrt{2_2J}-\sigma'_m$ space can be determined by Eqs. (20) and (21), corresponding to the value of plastic strain. Next, the f-function which is considered to be a dynamic yield function will be determined by Fig. (3). f is given by Eq. (22) corresponding to Fig. (3).

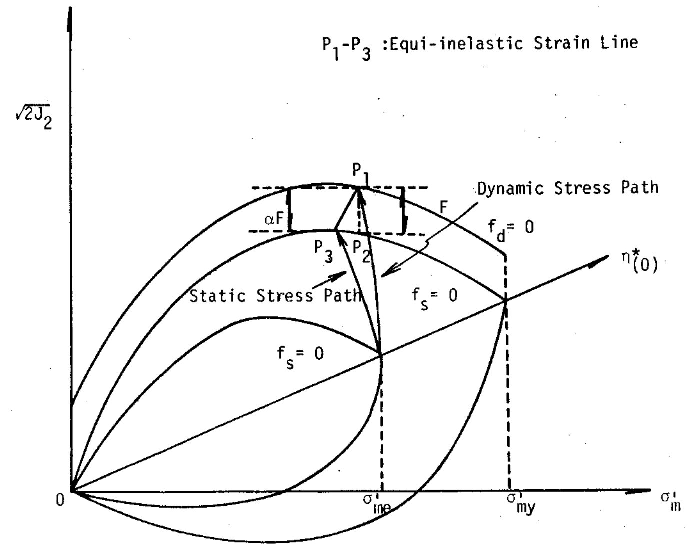

Fig. 3 Manner to determine f-function.

$$f=\sqrt{2J_2}-\eta^*_{(0)}\sigma'_m+M^*\sigma'_m\ln(\sigma'_m/\sigma'_{my})-F=0 \tag{22}$$

From the constitutive theory of the elastic-viscoplastic body in this paper, the dynamic stress-strain relation is expressed by

$$\dot{\varepsilon}_{ij}=\frac{1}{2G}\dot{s}_{ij}+\frac{1}{3}\gamma_2\dot{\sigma}'_m\delta_{ij}+o_{ijkl}\frac{\partial f}{\partial\sigma_{kl}} \tag{23}$$

The elastic strain-rate is given by

$$\dot{\varepsilon}^e_{kk}=\gamma_2\dot{\sigma}'_m \tag{24}$$

Taking account of the e-ln σ'_m curve of the consolidation, γ_2 is given by

$$\gamma_2=\frac{\kappa}{(1+e)\sigma'_m} \tag{25}$$

o_{ijkl} in Eq. (23) is assumed to be as

$$o_{ijkl}=\frac{\beta_2}{2}(\delta_{ik}\delta_{jl}+\delta_{il}\delta_{jk}) \tag{26}$$

Differentiating Eq. (22) with respect to the stress tensor, we obtain

$$\frac{\partial f}{\partial\sigma_{ij}}=\frac{s_{ij}}{\sqrt{2J_2}}+\left[M^*-\frac{\sqrt{2J_2}^{(s)}}{\sigma'^{(s)}_m}+M^*\ln\{\sigma'_m/\sigma'^{(s)}_m\}\right]\frac{1}{3}\delta_{ij} \tag{27}$$

The explicit expression of Eq. (23) can be rewritten by substituting this equation into Eq. (23) and by taking the relation of Eqs. (25) and (26) with the assumption that $\beta_1=\beta_2$,[1]

$$\dot{\varepsilon}_{ij}=\frac{\kappa}{(1+e)\sigma'_m}\dot{\sigma}'_m\frac{1}{3}\delta_{ij}+\frac{1}{2G}\dot{s}_{ij}+\frac{s_{ij}}{\sqrt{2J_2}}\beta_1+$$
$$+\beta_1\left[M^*-\frac{\sqrt{2J_2}^{(s)}}{\sigma'^{(s)}_m}+M^*\ln\{\sigma'_m/\sigma'^{(s)}_m\}\right]\frac{1}{3}\delta_{ij} \tag{28}$$

where

$$\beta_1=C_1\exp\left[m\frac{(q-q_s)}{\sigma'_{me}}\right]^{1)} \tag{29}$$

From Eq. (28), we obtain

$$\frac{\partial\varepsilon_{12}}{\partial t}=\frac{1}{2G}\frac{\partial\sigma'_{12}}{\partial t}+\beta_1(F)\frac{\sigma'_{12}}{\sqrt{2J_2}} \tag{30}$$

$$\frac{\partial\varepsilon_{kk}}{\partial t}=\frac{\kappa}{(1+e)\sigma'_m}\frac{\partial\sigma'_m}{\partial t}+$$
$$+\beta_1(F)\left[M^*-\frac{\sqrt{2J_2}^{(s)}}{\sigma'^{(s)}_m}+M^*\ln\{\sigma'_m/\sigma'^{(s)}_m\}\right] \tag{31}$$

Since Eqs. (10), (11) and (30) formulate the system of quasilinear hyperbolic partial differential equations, the characteristics exist. Along the characteristics, these differential relations are given by

$$\text{Along}\quad dx/dt=\pm C,\quad d\sigma'_{12}=\mp\rho C dv_2-2G\beta_1(F)\frac{\sigma'_{12}}{\sqrt{2J_2}}dt \tag{32}$$

$$\text{Along}\quad dx/dt=0,\quad d\varepsilon_{12}=\frac{1}{2G}d\sigma_{12}+\beta_1\frac{\sigma'_{12}}{\sqrt{2J_2}}dt \tag{33}$$

Fig. 4 shows the characteristics net. When the particle velocities at two points, B_0 and B_1, on the boundary of the bed rock are known, the stress and strain at C_0 can be determined by the differential relations along the lines B_0—B_1 and C_0—B_1.

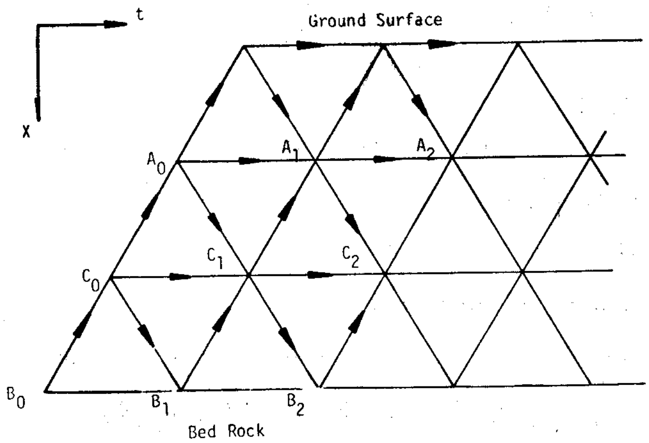

Fig. 4 Characteristics net.

The stress, strain and velocity at point C_2 can be obtained by solving the three differential relations along the lines (A_1—C_2, C_1—C_2 and B_2—C_2).
Along the line A_1—C_2, the relation is given

$$\sigma'_{12(C_2)} - \sigma'_{12(A_1)} = \rho\, C\,(v_{2(C_2)} - v_{2(A_1)}) - \\ -2G\beta_1 \frac{\sigma'_{12}}{\sqrt{2J_2}}(t_{(C_2)} - t_{(A_1)}) \tag{34}$$

Along the line C_1—C_2,

$$\varepsilon_{12(C_2)} - \varepsilon_{12(C_1)} = \frac{1}{2G}(\sigma'_{12(C_2)} - \sigma'_{12(C_1)}) + \\ + \beta_1 \frac{\sigma'_{12}}{\sqrt{2J_{2(C_1)}}}(t_{(C_2)} - t_{(C_1)}) \tag{35}$$

Along the line B_2—C_2,

$$\sigma'_{12(C_2)} - \sigma'_{12(B_2)} = -\rho\, C\,(v_{2(C_2)} - v_{2(B_2)}) - \\ -2G\beta_1 \frac{\sigma'_{12}}{\sqrt{2J_{2(B_2)}}}(t_{(C_2)} - t_{(B_2)}) \tag{36}$$

From Eqs. (34) and (36), $\sigma'_{12(C_2)}$ and $v_{2(C_2)}$ are determined and $\varepsilon_{12(C_2)}$ is obtained by Eq. (35). Conversely, if the stress, strain and velocity at points A_1, A_2 and C_1 are known, the stress, strain and velocity at point C_2 can be obtained theoretically. By the same manner, the underground motion can be presumed from the surface motion.

4. Numerical Examples and Discussion

In this section, we will examine the underground motion, using Eqs. (32) and (33) from the surface record. At the boundary of the layers, the mean value of parameters in two layers was used for the finite difference method.

Example A

Table 1 shows the parameters of the ground employed in example A. An elastic

Table 1 Parameters of example A.

Layer	H	G	ρ	C_1	
1	3.0	440	196	0	Elastic layer
2	3.1	480	200	0	
3	3.2	520	204	0	
4	3.28	560	208	10^{-6}	Clay Layer
5	3.36	600	212	10^{-5}	
6	36.12	640	216	10^{-4}	

H; depth (m)
G; Shear modulus (kg/cm^2)
ρ; density ($kg\ sec^2/m^4$)
C_1; parameter in Eq. (29) (1/sec)

layer of dry sand 9.3 m thick lies on the horizontal saturated clay layer. The clay layer is 42.3 m thick. The parameter m in Eq. (29) can be assumed to be as follows from the constant strain-rate triaxial compression test,

$$\begin{aligned} m&=49 && (|\varepsilon_{12}|\leq 10^{-3}) \\ m&=49-(|\varepsilon_{12}|-10^{-3})\times 10^{3} && (10^{-2}\geq|\varepsilon_{12}|\geq 10^{-3}) \\ m&=40 && (|\varepsilon_{12}|\geq 10^{-2}) \end{aligned} \tag{37}$$

where m depends on the amplitude of strain. The void ratio is calculated from the variation of the density with the depth. The other parameter K_0, M^*, λ and κ are taken as $K_0=0.5$, $M^*=1.4$, $\lambda=0.127$ and $\kappa=0.021$. The time trace of velocity on the surface is assumed to be sinusoidal and expressed by

$$v_{2(0)}=A_0\sin(2\pi ft), A_0=0.15\text{m/sec}, f=1.0 \tag{38}$$

Fig. 5 represents the calculated stress-strain relation at the depth of 33.1 m in the ground. In this figure, the viscoplastic strain is produced and the hysterisis damping loop can be recognized. The velocity record at the depth of 50.4 m is shown in Fig. 6 by the solid line. It is obviously known, as would be anticipated, that the velocity on the surface is considerably amplified. The dotted line shows the velocity response, which has been calculated under an assumption that all the layers are linearly elastic. Comparing the two calculated results, it may be noted that the absolute value of velocity in the clay layer, which has been assumed to be elastic-viscoplastic in behavior, is greater than the result calculated under the assumption described above. The difference of the amplitude of these two cases gradually vanishes with time, similar to the tendency of the velocity response. The part marked on the time axis shown in Fig. 7 indicates the period when the state of stress of the clay layer is viscoplastic in behavior. Moreover, it may be noted that the magnitude of stress, at which the viscoplastic behavior initiates, increases with

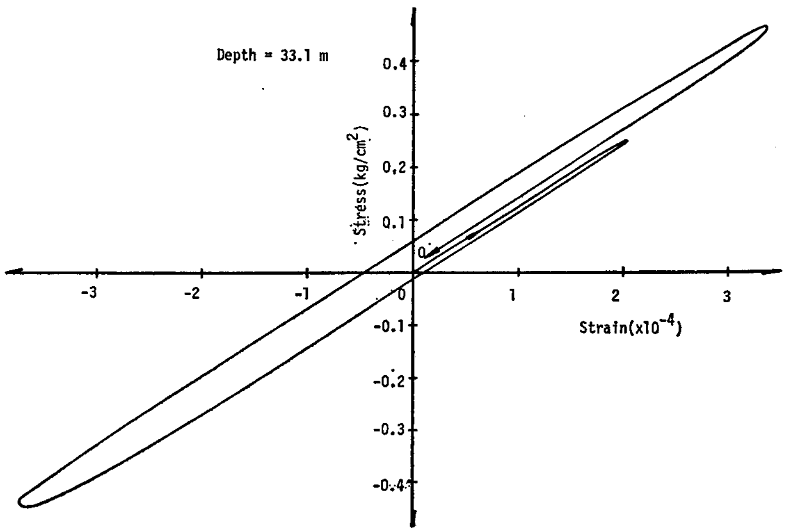

Fig. 5 Stress-strain relation (calculated result).

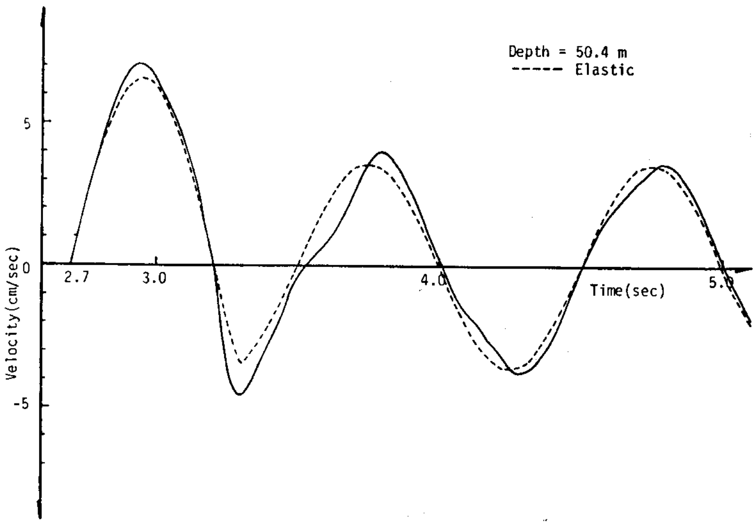

Fig. 6 Velocity response.

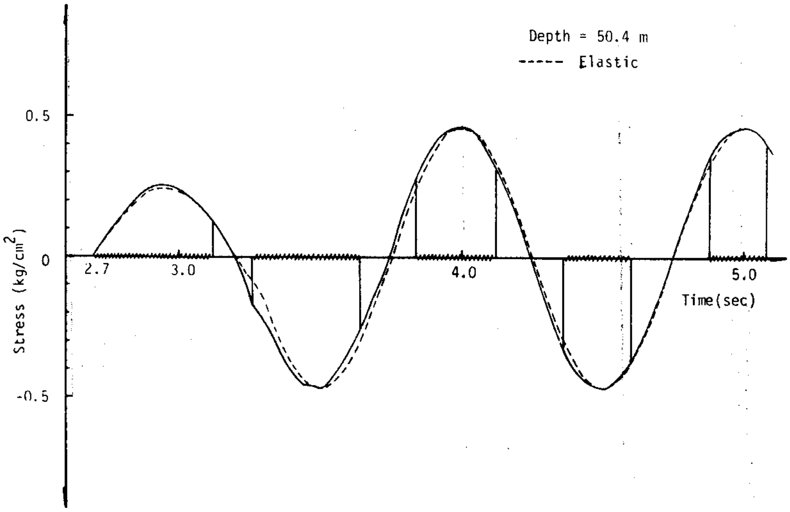

Fig. 7 Stress response.

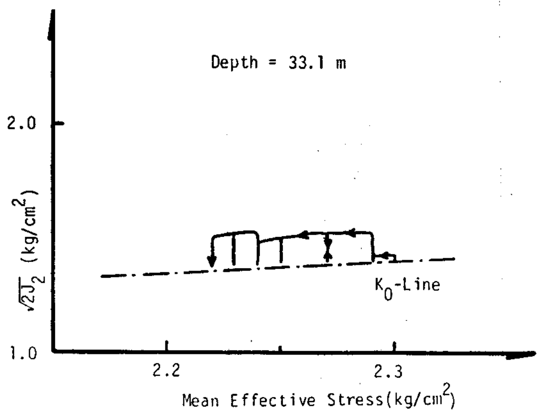

Fig. 8 Effective stress path (calculated resut).

the number of cycles repeated, caused by the hardening property of clay. Fig. 8 shows the typical effective stress path during the shear wave propagation. In this figure, the mean stress decreases and the residual pore pressure increases.

Example B

In example A, the sinusoidal velocity curve was used as a boundary condition, but for the practical aim of engineering, a more realistic wave propagation must be considered. Then, in this example, a seismic surface acceleration record was used as a boundary condition by transforming it into the velocity record. The frequency

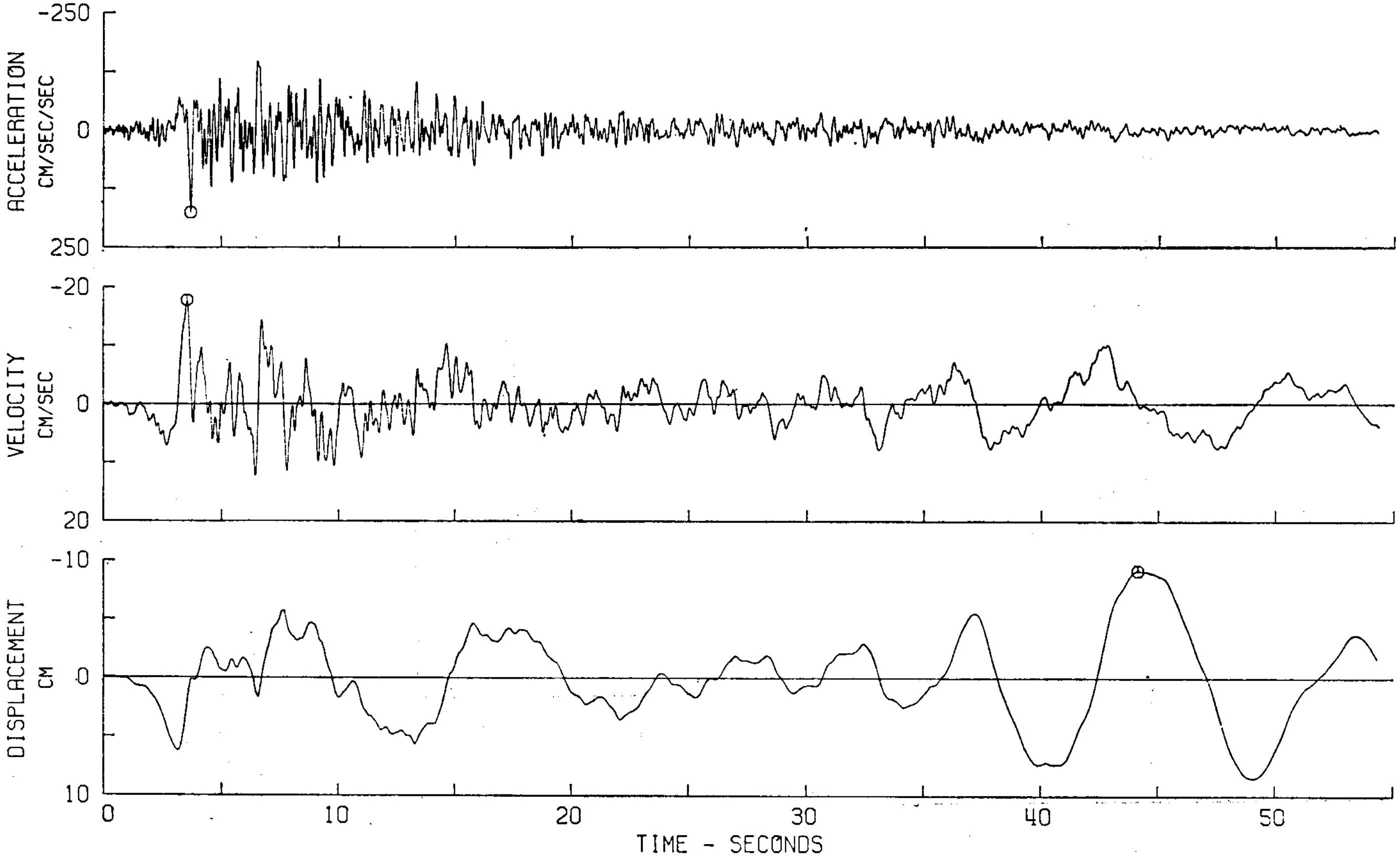

Fig. 9 S69E component of accelerogram at Taft during the 1952 Kern Country, California Earthquake.

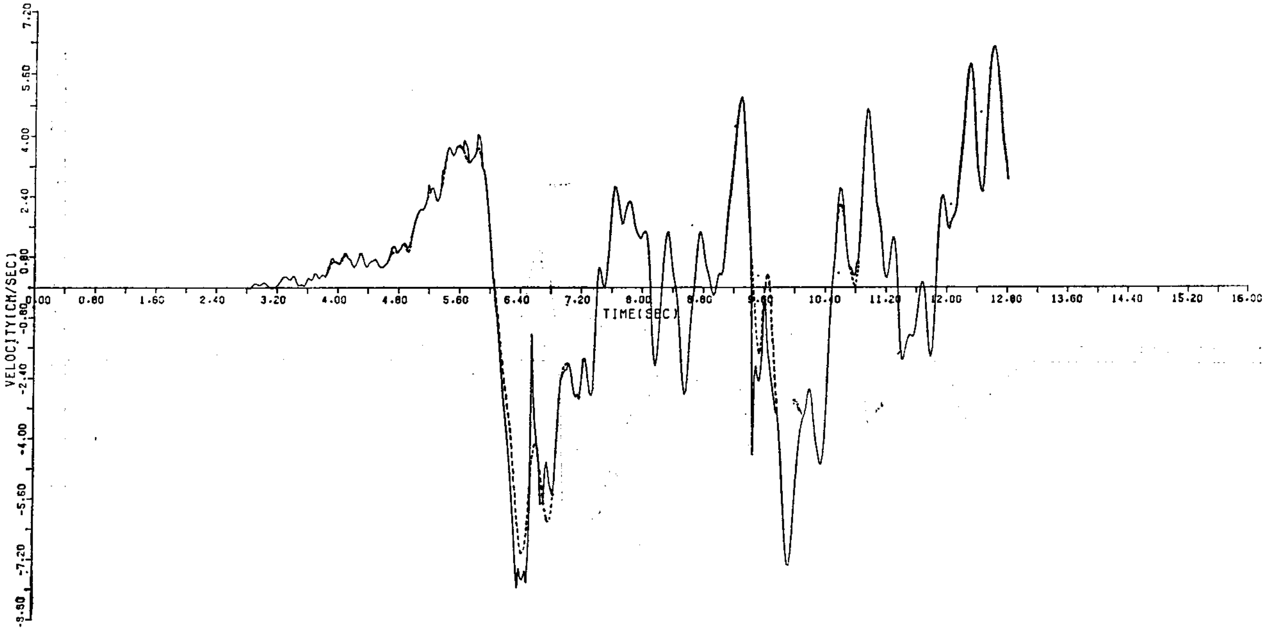

Fig. 10 Velocity response.

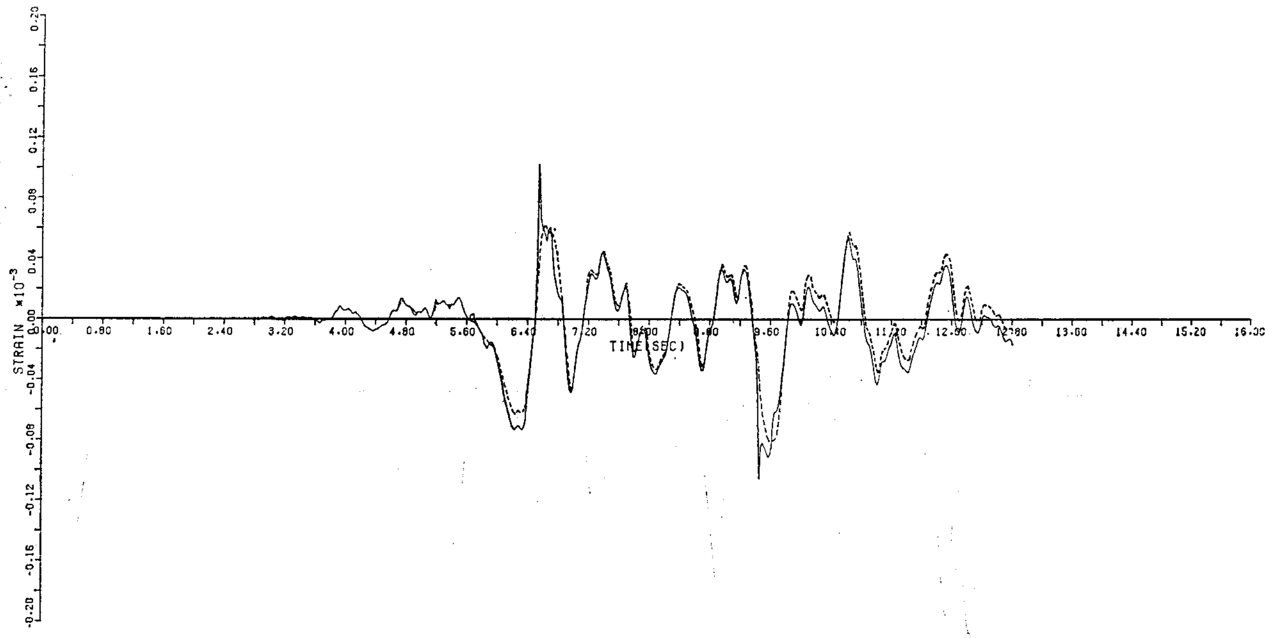

Fig. 11 Strain response.

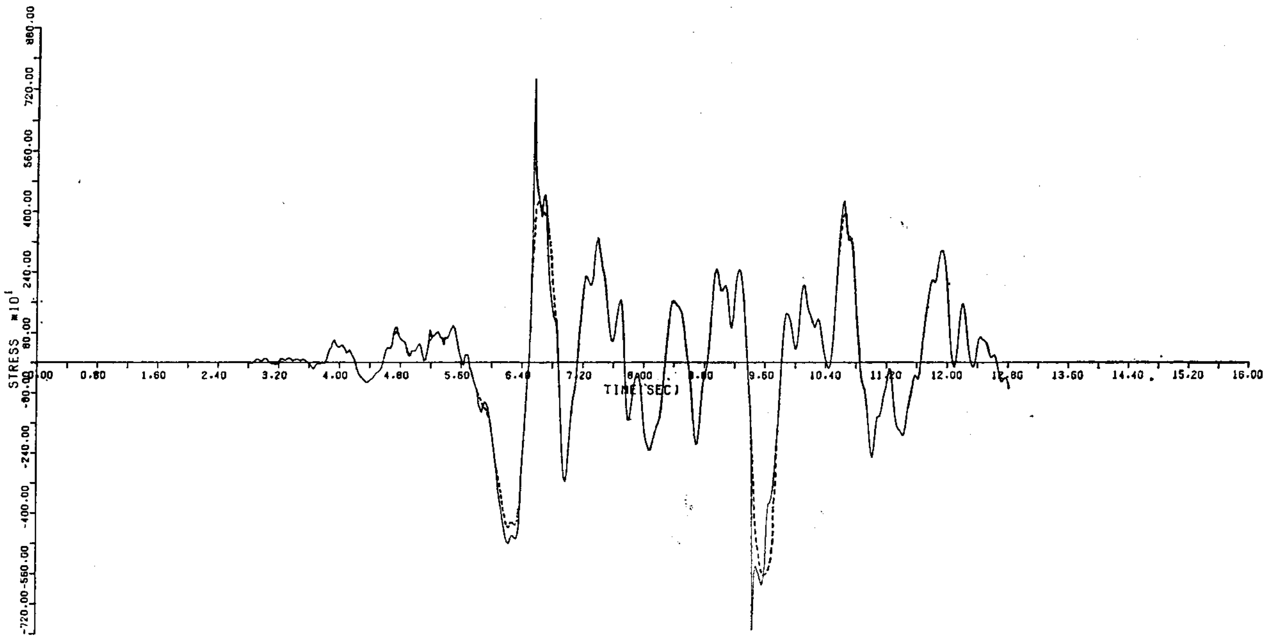

Fig. 12 Stress response.

Table 2 Parameters of example B.

Layer	H	ρ	C	C_1	m
1	4	196	200	0	0
2	4	200	200	0	0
3	4	204	200	0	0
4	6	208	300	10^{-4}	30
5	6	212	300	10^{-4}	30
6	104	216	400	10^{-4}	10

H: depth (m),
C: Shear wave velocity (m/sec)
ρ: density (kg sec^2/m^4)
C_1 parameter in Eq. (29) (1/sec)
m: parameter in Eq. (29)

component of the accelerogram more than 10 Hz was cut off by performing the base line correction. The first 10 sec of the S69E component of the accelerogram at Taft during the 1952 Kern Country, California Earthquake was used, as shown in Fig. 9. Table 2 shows the parameters of the ground employed in Example B. Fig. 10 shows the velocity response at the depth of 59.9 m, while the dotted line shows the result of the case where all the comprised layers are elastic. The solid line shows the result of the saturated elastic-viscoplastic ground. The velocity response for the elastic-viscoplastic ground is more predominant than that of the elastic ground in general. Fig. 11 represents the strain response and Fig. 12 shows the stress response at the depth of 59.5 m. The maximum value of the stress and strain response for the elastic case is slightly smaller than that of the other case depicted by solid line. These phenomena can be interpreted that the wave energy dissipates during the wave propagation through an elastic-viscoplastic soil layer by producing an inelastic strain. Even if the surface velocity responses are equal, a larger stress, strain and velocity may be induced in the saturated clay layer than in the elastic ground. During 10 sec, the mean effective stress decreases by 0.04 kg/cm^2, in this case at the depth of 59.5 m.

5. Conclusion

The main concern of this paper is to solve various engineering problems as a boundary value problem using a realistic stress-strain relation of soil. In this paper, the author has presented the calculation of strain, stress and velocity induced in the subground during the shear wave propagation through clay layers. The clay layer is regarded as an elastic-viscoplastic body. The stress-strain relation under the isotropic consolidation was formally extended to the K_0-consolidated state so as to be applied for the anisotropic consolidation. Some researchers have investigated the effect of the non-linearity of soil on the motion of ground, but the effect of the non-linearity in the time range, in consideration of visco-plastic nature of soil, has seldom been examined. Comparing the motion of the elastic ground with that of the elastic-viscoplastic ground during the seismic wave propagation, the effect of the time dependency of the stress-strain relation was examined. At the same time, the development of the pore water pressure during earthquake motion was discussed. The method of characteristics was used because of its short time for computation and because of the easiness in taking a non-linearity of the material into analysis. The main conclusions obtained in this paper are as follows.

(1) The motion of the layered cohesive soil during an earthquake can be calculated by using the method of characteristics. In this paper, from the surface records, the velocity, stress and strain induced under the ground were calculated. The stress-strain relation of cohesive soil was extended to the K_0-consolidated state from that developed by author in order to apply it to the layered soil condition.

(2) The difference between the non-linear and the linear elastic analysis was noted for the calculated results. From these results, even if the surface response is the same between the elastic ground and elastic-viscoplastic ground, the stress strain and velocity responses of the elastic-viscoplastic ground are greater than those of the elastic ground. These response characteristics vary with time in which the hardening property of clay can be obviously recognized. The characteristics of response develope behavior with time.

(3) The pore water pressure developed during loading was estimated. From the example given, it is noted that the residual pore water pressure may be developed during an earthquake, but the absolute value of the pore water pressure is relatively small compared to consolidation pressure.

Acknowledgement

The author wishes to express his sincere thanks to Professor K. Akai of Department of Transportation Engineering and Professor K. Toki of the Disaster Prevension Research Institute of Kyoto University for their helpful discussions and constructive criticism.

References

1) Oka, F. Proc. of JSCE, No. 272, Apr., 117 (1978).
2) Constantious, I. V., J. M. Rosset and J. T. Christian, Proc. 5th WCEE, 1806 (1973).
3) Streeter, V. L., E. B. Wylie and F. E. Richart Jr., Journal Geotechnical Engineering Division, A. S. C. E., Vol. 100, No. GT3, 247 (1974).
4) Idriss, I. M. and H. B. Seed, Journal of the Soil Mechanics and Foundation Division, A. S. C. E., Vol. 94, No. SM4, 1003 (1968).
5) Richart, F. E., Jr. and E. B. Wylie, Symposium, Structure and Geotechnical Mechanics, Univ. of Illinois, Urbana, Illinois, Oct., 2 (1975).
6) Adachi, T. and M. Okano, Soils and Foundations, Vol. 14, No. 4, 55 (1974).